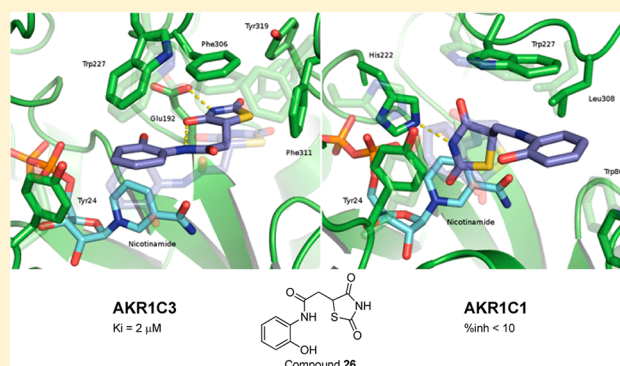


Selective Inhibitors of Aldo-Keto Reductases AKR1C1 and AKR1C3 Discovered by Virtual Screening of a Fragment Library

Petra Brožič,^{†,⊥} Samo Turk,^{‡,⊥} Adegoke O. Adeniji,[§] Janez Konc,^{||} Dušanka Janežič,^{||} Trevor M. Penning,[§] Tea Lanišnik Rižner,[†] and Stanislav Gobec^{*,‡}[†]Institute of Biochemistry, Faculty of Medicine, University of Ljubljana, Vrazov trg 2, 1000 Ljubljana, Slovenia[‡]Faculty of Pharmacy, University of Ljubljana, Aškerčeva 7, 1000 Ljubljana, Slovenia[§]Center of Excellence in Environmental Toxicology, Department of Pharmacology, Perelman School of Medicine University of Pennsylvania, Philadelphia, Pennsylvania, United States^{||}National Institute of Chemistry, Hajdrihova 19, 1000 Ljubljana, Slovenia

S Supporting Information

ABSTRACT: Human aldo-keto reductases 1C1–1C4 (AKR1C1–AKR1C4) function in vivo as 3-keto-, 17-keto-, and 20-ketosteroid reductases and regulate the activity of androgens, estrogens, and progesterone and the occupancy and transactivation of their corresponding receptors. Aberrant expression and action of AKR1C enzymes can lead to different pathophysiological conditions. AKR1C enzymes thus represent important targets for development of new drugs. We performed a virtual high-throughput screen of a fragment library that was followed by biochemical evaluation on AKR1C1–AKR1C4 enzymes. Twenty-four structurally diverse compounds were discovered with low μM K_i values for AKR1C1, AKR1C3, or both. Two structural series included the salicylates and the *N*-phenylanthranilic acids, and additionally a series of inhibitors with completely novel scaffolds was discovered. Two of the best selective AKR1C3 inhibitors had K_i values of 0.1 and 2.7 μM , exceeding expected activity for fragments. The compounds identified represent an excellent starting point for further hit-to-lead development.



■ INTRODUCTION

Human aldo-keto reductases 1C1–1C4 (AKR1C1–AKR1C4) function in vivo as 3-keto-, 17-keto-, and 20-ketosteroid reductases to varying extents and thus regulate the activity of androgens, estrogens, and progesterone and the occupancy and transactivation of their corresponding receptors.^{1,2} Human members of the AKR1C subfamily share more than 86% sequence identity at the amino acid level and, interestingly, AKR1C1 and AKR1C2 differ in seven amino acid residues, only one of which (Leu/Val54) is in the active site.³ On the basis of the known crystal structures of AKR1Cs, differences in the substrate binding sites have been identified⁴ and the binding sites for substrates/inhibitors have been characterized.

Aberrant expression and action of AKR1C enzymes can lead to different pathophysiological conditions.^{5,6} For instance, in the endometrium, both AKR1C1 and AKR1C3 prevent the progestational and pro-differentiating effect of progesterone in the uterus and the ectopic endometrium.^{7,8} Thus inhibitors of these enzymes could help maintain pregnancy and may have a role in the treatment of endometriosis. Increased expression of AKR1C3 can result in high levels of the potent androgens, testosterone and dihydrotestosterone in the prostate or the potent estrogen estradiol in the breast, leading to enhanced

proliferation of prostate or breast cells.^{9,10} Thus inhibitors of AKR1C3 could be used in antihormonal therapy of prostate and breast cancer. In the prostate, on the other hand, AKR1C1 and AKR1C2 convert the most potent androgen 5 α -dihydrotestosterone to pro-apoptotic 5 α -androstane-3 β ,17 α -diol and 5 α -androstane-3 α ,17 α -diol, respectively.^{11,12} These data suggest a need for selective inhibitors for AKR1C1 and AKR1C3. Inhibition of AKR1C2 and liver-specific AKR1C4, which are both involved in inactivation of steroid hormones and their elimination from the body, is not desirable.

In the past decade, steroidal and nonsteroidal AKR1C inhibitors have been reported.^{4,13,14} Several compounds with K_i values in the nanomolar range for AKR1C1 and AKR1C3 have been recently found based on the observation that salicylates were potent and selective inhibitors for AKR1C1 and that *N*-phenylanthranilates were nonselective but potent inhibitors of the AKR1C enzymes.^{15,16} Thus, among salicylic acid derivatives, 3-bromo-5-phenylsalicylic acid with a K_i value of 4.1 nM for AKR1C1 showed 20-fold specificity for AKR1C1 compared to AKR1C2 and more than 100-fold specificity when

Received: March 9, 2012

Published: August 13, 2012

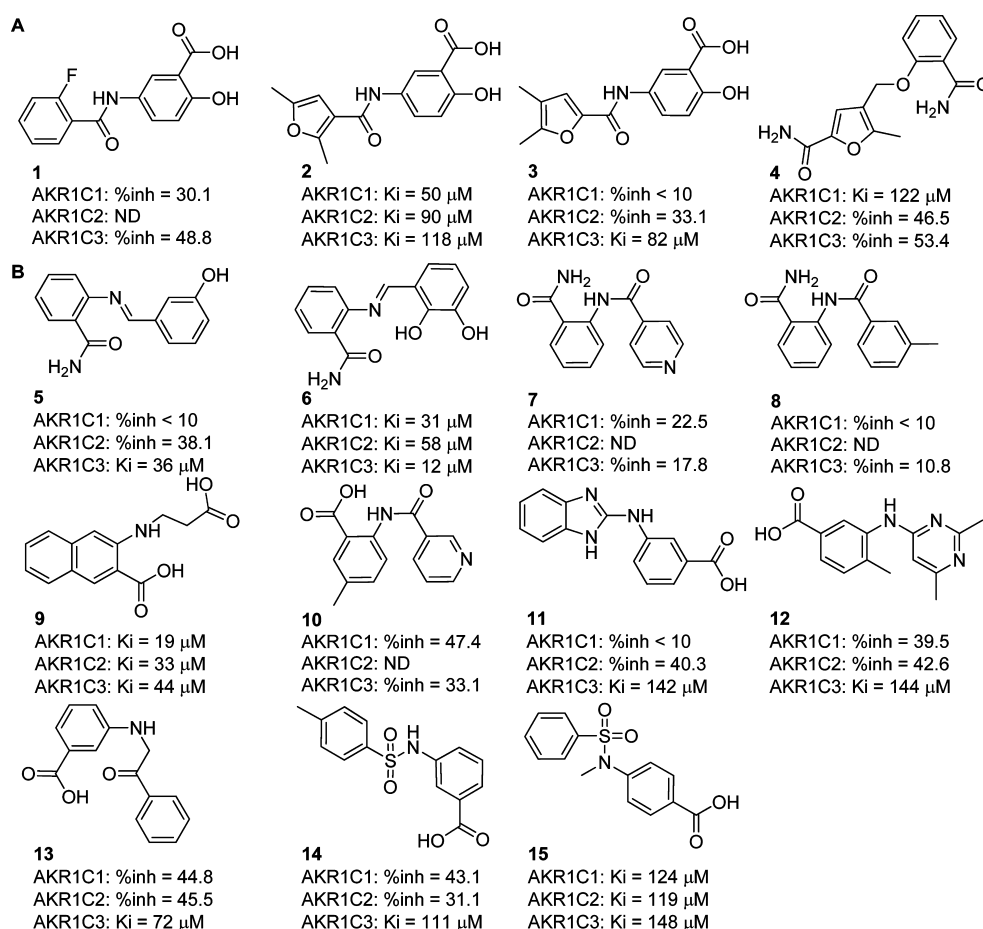


Figure 1. Structures and AKR1C1–3 inhibitory activities of salicylic acid (A) and aminobenzoic acid (B) derivatives. Percent inhibition was determined at 400 μ M inhibitor concentration.

compared to AKR1C3 and AKR1C4.^{13,14,17–19} Similarly, *N*-phenylaminobenzoates based on flufenamic acid, in which the bridge amine and the carboxylate are *meta* to one another and an electron-withdrawing group was placed in the *N*-phenyl ring, produced compounds with nanomolar affinity and high selectivity for AKR1C3.^{20,21}

Crystal structures of all AKR1C isozymes have been resolved,^{4,7,13} and several computational structure-based studies have been performed recently, leading to identification of new structures with low μ M and nM affinities.^{22,23} In addition to these methods, fragment-based drug discovery has evolved as an important alternative methodological approach. Fragments are defined as low molecular weight, moderately lipophilic, highly soluble organic molecules (MW < 300; log *P* < 3), which typically bind to their target with micro- to millimolar affinity. These fragments can be further modified by adding additional functional groups to yield potent high affinity lead molecules.²⁴ Despite the high potential of this fragment-based approach, no such study has yet been performed in the search for inhibitors of AKR1C isozymes. In this paper, we describe the virtual high-throughput screening of a fragment library followed by biochemical evaluation on target aldo-keto reductases AKR1C1–C4. Twenty-four structurally diverse compounds were discovered with low μ M K_i values for therapeutically relevant AKR1C1, AKR1C3, or both. Two of the best selective AKR1C3 inhibitors had K_i values of 0.1 and 2.7 μ M, exceeding the expected activity for fragments.

RESULTS AND DISCUSSION

Virtual Screening. For our study, compounds from suppliers Asinex, ChemBridge, Maybridge, and the U.S. National Cancer Institute (NCI) were selected and downloaded from the ZINC database,²⁵ yielding 1.9 million compounds. Because of the size of this bank of compounds and the possibility that it contains compounds with unwanted properties, a filtering procedure was applied to provide a more focused library. Filtering was based on simple molecular descriptors, selection of which was based loosely on fragment-based rules.²⁶ Additional filters were used to eliminate potentially problematic compounds, so all compounds with reactive functional groups were eliminated together with all known and predicted aggregators.²⁷ Out of 1.9 million compounds, 143000 compounds remained. Docking experiments were carried out with FlexX 3.1 (BiosolveIT GmbH).²⁸ Active sites for AKR1C1 and AKR1C3 were defined as the portion of the enzyme within 6 Å from respective cocrystallized ligands. All of the 143000 compounds that passed the filtering procedure were docked into active site of AKR1C1 and AKR1C3 and ranked according to the score of the best scored conformation. To ensure binding with the catalytic Tyr55, for both docking experiments, an essential interaction was defined, so that only docked conformations with an H-bond acceptor no more than 3 Å from Tyr55 were considered. From the highest ranked compounds from each docking experiment, 37 available compounds for AKR1C1 (Supporting Information Table 1, compounds S1–S37) and 33 available compounds for AKR1C3

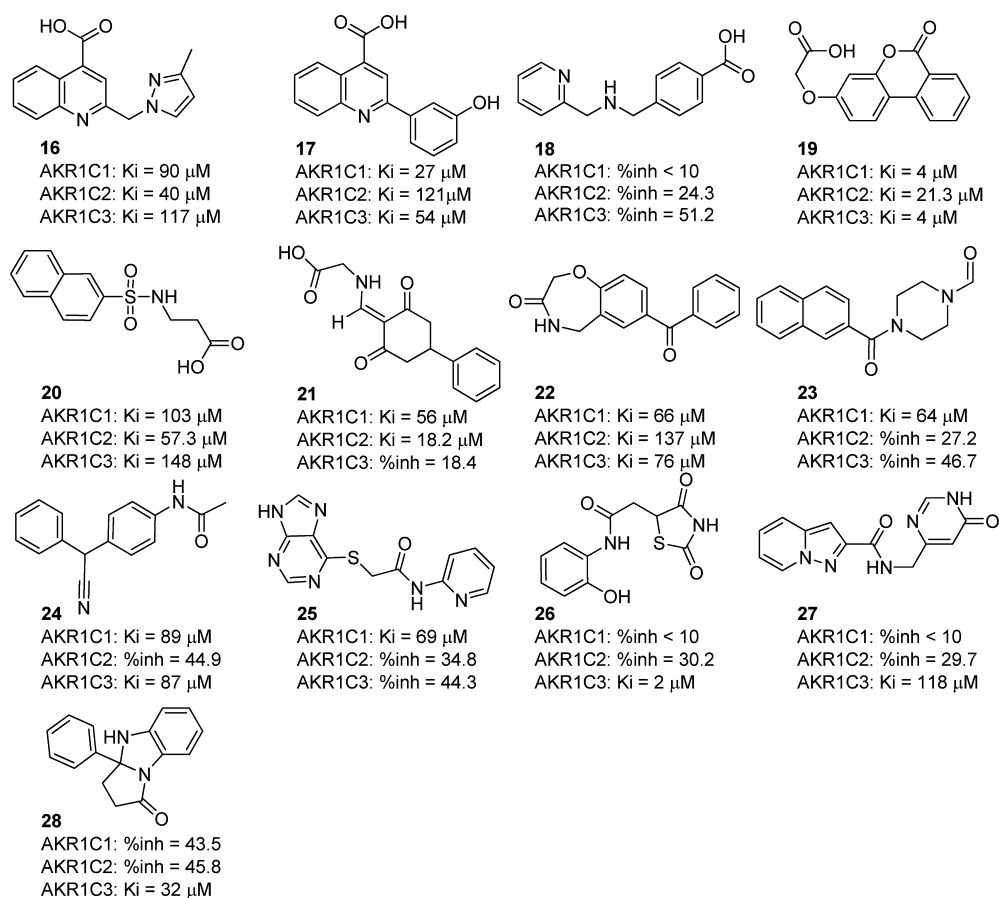


Figure 2. Structures and inhibitory activities of AKR1C1–AKR1C3 inhibitors with novel scaffolds. Percent of inhibition was determined at $400 \mu\text{M}$ inhibitor concentration.

(Supporting Information Table 1, compounds S38–S70) were obtained for in vitro evaluation. Among these hits there were some new inhibitors, anthranilic acid and salicylic acid derivatives, with scaffolds that are known to inhibit AKR1C enzymes,^{16,23,29} which validates our method and is supported by the successful redocking of cocrystallized inhibitors with high scores.

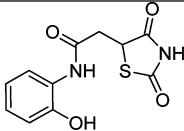
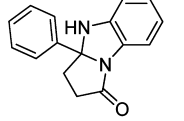
Biochemical Evaluation of Hits Against AKR1C1–AKR1C4. Out of 70 obtained compounds, 11 compounds were insoluble. For the other 59 compounds, the percentage of inhibition of AKR1C1 and AKR1C3 at compound concentrations of $400 \mu\text{M}$ was first determined. All compounds, regardless of the virtual screen in which they were identified, were assayed on both AKR1C1 and AKR1C3 enzymes because these enzymes share 88% identical amino acid residues and thus have a common fold and similar active site. In addition, we were interested to learn if it is possible to discover isoform selective AKR1C inhibitors by virtual screening. For compounds that showed more than 55% inhibition of AKR1C1 and/or 55% inhibition of AKR1C3, IC_{50} values were determined and selectivity toward AKR1C2 was measured. The complete results of the biochemical characterization are presented in Supporting Information Table 1. In the case of the most promising compounds, further kinetic analysis was pursued.

Salicylic Acid and Aminobenzoic Acid Derivatives. In a series of salicylic acid derivatives (Figure 1A), compounds 1, 2, and 3 are 5-aminosalicylates with different acyl substituents on the amino group. Compound 1, 5-(2-fluorobenzamido)salicylic

acid, shows only low and moderate inhibition of AKR1C1 and AKR1C3, respectively. Replacement of 2-fluorobenzoyl moiety with dimethylfurancarboxyl as in compounds 2 and 3 significantly improved AKR1C1–3 inhibition. It appears that the methylation pattern of the furan ring together with the position of carbonyl substituent influences inhibition and selectivity. Compound 2, 5-(2,5-dimethylfuran-3-carboxamido)salicylic acid, is a nonselective AKR1C1–3 inhibitor, with K_i values of 50, 90, and $118 \mu\text{M}$ on AKR1C1, AKR1C2, and AKR1C3, respectively. On the other hand, compound 3, 5-(4,5-dimethylfuran-2-carboxamido)salicylic acid, is a selective AKR1C3 inhibitor with K_i value of $82 \mu\text{M}$ on AKR1C3, very low inhibition of AKR1C2, and no observable inhibition of AKR1C1. Another salicylic acid derivative, compound 4 (4-((2-carbamoylphenoxy)methyl)-5-methylfuran-2-carboxamide) is partially selective toward AKR1C1 with K_i value of $122 \mu\text{M}$ and a moderate inhibitor of AKR1C2 and AKR1C3.

Compounds 5–10 (Figure 1B) belong to the group of 2-aminobenzoic acids (anthranilic acid derivatives). Compounds 5 and 6 are both 2-(benzylideneamino)benzamides which differ only by one aromatic hydroxyl group. Compound 5, 2-(3-hydroxybenzylideneamino)benzamide, is a selective AKR1C3 inhibitor, whereas compound 6, 2-(2,3-dihydroxybenzylideneamino)benzamide, inhibits AKR1C1–AKR1C3 to the same extent in the low micromolar concentration range. With a $K_i = 12 \mu\text{M}$, compound 6 is also the best AKR1C3 inhibitor from the salicylic and aminobenzoic acid series. The *N*-acyl anthranilamides 7 and 8 had only low inhibitory effect on AKR1C enzymes. On the other hand, the naphthalene analogue

Table 1. Selectivity of Inhibitors 26 and 28 Evaluated with Fluorescence-Based Assay

Compound	Structure	AKRIC1	AKRIC2	AKRIC3	AKRIC4
26		inh = 37% (300 μM conc)	IC ₅₀ = 205.7 μM K _i * = 102.8 μM	IC ₅₀ = 0.213 μM K _i * = 0.107 μM	inh = 35% (300 μM conc)
28		IC ₅₀ = 167.2 μM K _i * = 83.6 μM	IC ₅₀ = 92.3 μM K _i * = 46.2 μM	IC ₅₀ = 5.46 μM K _i * = 2.73 μM	inh = 48% (300 μM conc)

*K_i estimated on the assumption that inhibition type is competitive.

of the anthranilic acid **9**, 3-(2-carboxyethylamino)-2-naphthoic acid, is a potent inhibitor of AKRIC1–3, and with a K_i value of 19 μM is also the best inhibitor of AKRIC1 in the series of salicylic and aminobenzoic acid derivatives. *N*-Acyl anthranilic acid **10** is, similar to the *N*-acyl anthranilamides **7** and **8**, only a weak inhibitor of AKRIC1 and AKRIC3.

The 3-aminobenzoic acids **11–14** (Figure 1B) are all selective AKRIC3 inhibitors with micromolar K_i values between 77 μM and 144 μM. A comparison of the activities of 3-aminobenzoic acids **11–14** with structurally related derivatives of 5-aminosalicylic acid **1–3** shows that 3-aminobenzoic acids have comparable or better AKRIC3 inhibitory activities and superior selectivity toward this isoform. The only 4-aminobenzoic acid derivative identified by this screening, compound **15**, 4-(*N*-methylphenylsulfonamido)benzoic acid, is a nonselective micromolar AKRIC1–3 inhibitor.

Out of 25 active compounds with better than 55% inhibition of either AKRIC1 or AKRIC3 in initial screening, 11 are either derivatives of salicylic acid (compounds **2–4**) or of aminobenzoic acid (compounds **5**, **6**, **9**, and **11–15**). Four additional derivatives of salicylic acid or aminobenzoic acid (compounds **1**, **7**, **8**, and **10**) have moderate or low inhibition of AKRIC enzymes, and one compound, **S50**, was insoluble (Supporting Information Table 1).

Both salicylic and aminobenzoic acid derivatives are well-known inhibitors of AKRIC1–4 enzymes, with activities in the low micromolar and nanomolar range. Extensive work was done on NSAIDs with these scaffolds, and the highest inhibitory activity was observed in case of mefenamic acid (K_i (AKRIC1, AKRIC2, AKRIC3) = 0.81, 0.22, 0.30 μM).¹⁶ Compounds **1–15** represent new inhibitors, which are according to similarity calculations structurally different to known inhibitors with the same scaffolds (Supporting Information Table 2). Compounds **1–15** thus cover until now unexplored chemical space and provide new information about the structure–activity relationship of this series.

Other Structural Classes. Other active compounds belong to different structural classes (Figure 2) whose scaffolds have not been reported to date as inhibitors of AKRIC enzymes. The best inhibitors of AKRIC1 and AKRIC3 reported here are from this series, and they represent excellent starting points for development of new selective AKRIC1/3 inhibitors. Interestingly, eight out of 14 compounds from this series were identified with virtual screening on AKRIC3, although, as discussed above, this does not necessarily mean that they exhibit preferential AKRIC3 inhibitory activity.

Compounds **16–21** all have a carboxylic acid functional group, share low isoform selectivity, and are inhibitors of at

least two AKRIC isoforms. Compounds **16**, 2-((3-methyl-1*H*-pyrazol-1-yl)methyl)quinoline-4-carboxylic acid, and **17**, 2-(3-hydroxyphenyl)quinoline-4-carboxylic acid, are both quinoline derivatives with different substituents at position 2. The change from 3-hydroxyphenyl substituent to 3-methylpyrazol-1-yl increases AKRIC2 inhibitory activity and, concurrently, reduces slightly the inhibition of the other two AKRIC isoforms. Compounds **18–21** are structurally unrelated. Compound **18**, 4-(((pyridin-2-ylmethyl)amino)methyl)benzoic acid, is only a low and moderate inhibitor of AKRIC2 and AKRIC3, respectively. Compound **19**, 2-((6-oxo-6*H*-benzo[*c*]chromen-3-yl)oxy)acetic acid, while nonselective, is the best inhibitor of AKRIC1 (K_i = 4 μM) and second best inhibitor of AKRIC3 (K_i = 4 μM) reported here. Compound **20**, 3-(naphthalene-2-sulfonamido)propanoic acid, is also a nonselective inhibitor of AKRIC1–3 enzymes. On the other hand, compound **21**, 2-(((2,6-dioxo-4-phenylcyclohexylidene)methyl)amino)acetic acid, is a good inhibitor of AKRIC1 and also the best inhibitor of AKRIC2 (K_i = 18.2 μM) reported here. Interestingly, it is a poor inhibitor of AKRIC3.

Compounds **22** and **23** have either an aldehyde or ketone functional group. Compound **22** is a nonselective AKRIC1–3 inhibitor, while compound **23**, 4-(2-naphthoyl)piperazine-1-carbaldehyde, is AKRIC1 selective with K_i value of 64 μM. The remaining compounds, **24–28**, have no common structural motif, and with the exception of compound **24**, all show selectivity for only one of the AKRIC isoforms. Compound **24**, *N*-(4-(cyano(phenyl)methyl)phenyl)acetamide, inhibits AKRIC1 and AKRIC3 in roughly the same range, with K_i values in both enzymes of just under 90 μM and is only a moderate inhibitor of AKRIC2. Compound **25**, 2-((9*H*-purin-6-yl)thio)-*N*-(pyridin-2-yl)acetamide, is a selective AKRIC1 inhibitor with K_i value of 69 μM. On the other hand, compounds **26**, **27**, and **28** are all selective AKRIC3 inhibitors. Compound **27**, *N*-((6-oxo-1,6-dihydropyrimidin-4-yl)methyl)pyrazolo[1,5-*a*]pyridine-2-carboxamide, is a good inhibitor of AKRIC3 with a K_i value of 118 μM, but the most interesting members of this group of compounds, due to their good AKRIC3 inhibition (K_i values of 2 and 32 μM, respectively) and very good selectivity, are compounds **26** and **28** (see below). Both these compounds contain five-membered heterocyclic rings, which can hypothetically mimic the cyclopentane ring of prostaglandin, a natural substrate of AKRIC3.

Selectivity toward AKRIC4. Two of the most potent and AKRIC3-selective inhibitors, compounds **26** and **28**, were also counterscreened against the liver specific enzyme, AKRIC4, by following the oxidation of *S*-tetralol in the presence of NADP⁺.

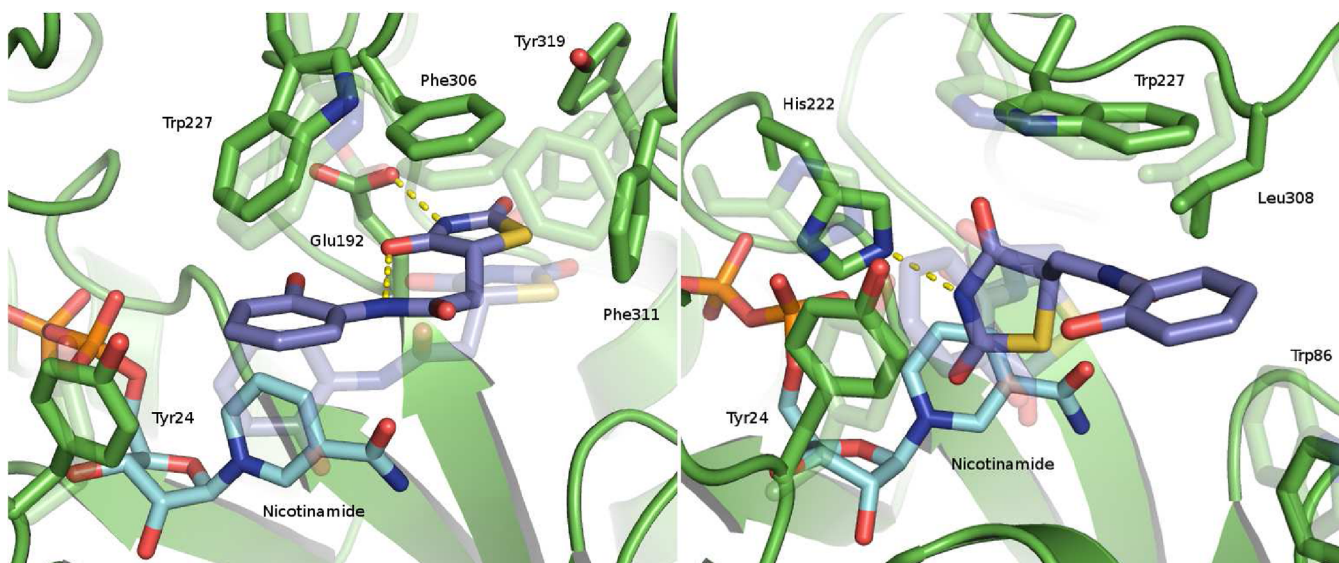


Figure 3. Compound **26** in the binding sites of AKR1C3 (left) and AKR1C1 (right). Molecules after 10 ns of molecular dynamics simulations are opaque; before dynamics, they are transparent. Binding sites are superimposed using ProBiS web server.³³ Compound **26** is violet, NADP⁺ cofactor is cyan, and H-bonds are yellow dashes.

To enable a proper comparison, the potency of these two compounds against other AKR1C enzymes was determined using the same enzyme assay. These results are shown in Table 1.

Compound **26** is a potent and selective inhibitor of AKR1C3 (Table 1). It is about 1000-times more selective for AKR1C3 over AKR1C2, and selectivity is even higher when compared with AKR1C1 and AKR1C4. Compound **28** is less selective; it has 17-fold and 30-fold selectivity against AKR1C2 and AKR1C1, respectively, and much higher selectivity against AKR1C4. Interestingly, we observed higher potency of these two compounds with the substrate *S*-tetralol and coenzyme NADP⁺ at pH 7.0 (Table 1), as compared to measurement of the inhibition of 1-acenaphthenol oxidation in the presence of NAD⁺ at pH 9.0 (Table 1). These differences in affinities are consistent with the finding that AKR1C enzymes display higher affinity for substrates and inhibitors when NADP(H) is bound and assays are performed at pH 7.0.³⁰

Molecular Dynamics. The selectivity of compound **26** for AKR1C3 could not be explained by docking, which predicted the inhibition of isoform AKR1C1 (docking rank 51) but not of AKR1C3 (docking rank 21509). Therefore, to determine if an induced fit is possible upon binding, we performed two 10 ns molecular dynamics simulations of compound **26** bound to AKR1C1 and AKR1C3, starting each dynamics with the best-scored pose for that isoform (Figure 3).

Although molecular dynamics is a theoretical experiment, the simulation shows that binding of compound **26** to AKR1C3 could induce conformational changes to both inhibitor and enzyme (Figure 3, left). After the dynamics, the compound presumably assumes a stable, energetically favored, planar conformation, with an estimated free energy of binding of -5 kcal/mol, whereas the docked pose had $+4$ kcal/mol (both binding energies estimated by AutoDock scoring).³¹ Most changes in compound **26** that occur during simulation are in the phenol ring with an associated amide group, which rotates by about 90° , presumably allowing an intramolecular H-bond to form between oxygen of the thiazolidinedione moiety and hydrogen of the amide group. The resulting planar con-

formation of the molecule, in which thiazolidinedione and phenol rings are coplanar, presumably enables the phenol to form π -stacking interactions with Tyr24, Trp227, and the nicotinamide moiety of NADP⁺. At the end of the simulation, the predicted pose of the phenol resembles that of the indole ring of indomethacin bound to AKR1C3 in the crystal structure 1S2A. After rearrangement of Phe306, Phe311, and Tyr319 residues, the thiazolidinedione ring could form π -stacking and hydrophobic interactions with these residues, which constitute the SP1 subpocket,¹⁴ and in addition, the thiazolidinedione moves further into this SP1 subpocket, potentially forming a H-bond with Glu192. Such H-bonds, located in sterically restricted and hydrophobic environments, are often strong, but their energy is difficult to determine by molecular modeling.³²

In AKR1C1 simulation, compound **26** presumably adopts a pose in which phenol ring is partially exposed to the solvent at the entrance to the binding site (Figure 3, right). During the simulation, the thiazolidinedione moiety remains stacked between Tyr24 and nicotinamide and, depending on the protonation state of His222, may form an H-bond with His222 with the nicotinamide amino group as the H-bond donor. The phenol ring shifts toward the Trp86 residue, which could allow it to form π -stacking interactions with Trp86 and Trp227. Interactions with the SP1 subpocket are not possible in this isoform, due to residues Leu306 and Leu308, which block the entrance to the subpocket. The calculated binding energy is between -4 to -5 kcal/mol throughout the simulation.

The selectivity of compound **26** for AKR1C3 is most likely due to the larger size of the SP1 subpocket which is composed of different residues compared to other isoforms.¹⁴ This enables a binding pose in AKR1C3 that is not possible in AKR1C1 and could not be predicted using docking alone. Upon binding of compound **26** to AKR1C3, induced conformational changes are predicted to occur, which expose additional interactions with the SP1 subpocket. Further design of inhibitors, selective for AKR1C3, should therefore focus on exploiting the differences in SP1 subpockets and demands accounting for conformational changes during the binding process.

Assessment of Virtual Screening Protocol. Out of 59 compounds assayed biochemically, 24 showed good inhibitory activities for either AKR1C1, AKR1C3, or both, which corresponds to a 34% hit-rate, given that 70 compounds were obtained from virtual screening. Three compounds were specific inhibitors of AKR1C1, 10 were specific for AKR1C3 and two inhibited both AKR1C1 and AKR1C3 but not AKR1C2. The decision to assay compounds from both virtual screenings with both AKR1C1 and AKR1C3 enzymes gave interesting insights into the ability of FlexX docking program to find selective inhibitors of the structurally closely related AKR1C enzymes. Out of 37 compounds obtained from virtual screening on AKR1C1 (Supporting Information compounds S1–S37), only one is a selective inhibitor of AKR1C1, and interestingly, seven compounds were actually selective for AKR1C3; four compounds show no isoform inhibition selectivity. On the other hand, out of the 33 compounds obtained from virtual screening on AKR1C3 (compounds S38–S70 in Supporting Information), three are selective inhibitors of AKR1C3, two inhibit AKR1C1 and show low or no inhibition of AKR1C3, and six are active but show no isoform selectivity. It is obvious from these results that our virtual screening protocol is capable of finding potent AKR1C inhibitors but is unable to predict the isoform selectivity.

CONCLUSIONS

We have used *in silico* screening of a fragment library to search for inhibitors of AKR1C1 and AKR1C3. Out of 70 compounds selected for biochemical evaluation, 24 (34%) had K_i values in the micromolar range for AKR1C1, AKR1C3, or both. Although our screening protocol was unable to predict which compounds are selective inhibitors for specific isoforms, three compounds were discovered that are selective for AKR1C1 and 10 are selective inhibitors of AKR1C3. Among new inhibitors discovered, 15 are inhibitors with known scaffolds (salicylic acid and *N*-aminobenzoic acid derivatives) and they provide additional information about structure–activity relationships for these two compound series. More importantly, 12 new structural classes of compounds were discovered that have until now not been reported to be inhibitors of AKR1C enzymes. As compounds with K_i values as low as 100 nM were identified before any structural optimization of the fragments, it is clear that the fragment-sized compounds identified have a great potential for development into drug candidates with higher molecular weight. Two hits discovered, compounds **26** and **28**, have high affinity for AKR1C3, show excellent selectivity, and represent a valuable starting point for further synthetic optimization and development of drug candidates for treatment of hormone dependent and independent forms of prostate and breast cancers.

EXPERIMENTAL SECTION

Computer Hardware. All of the computational procedures were carried out on two workstations. One workstation has four dual core AMD Opteron 2.0 GHz processors, 16 GB RAM, four 320 GB hard drives in a RAID10 array, and Nvidia GeForce 7900 graphic cards and runs the 64-bit Fedora 7. The second workstation has two quad core Intel Xeon 2.2 GHz processors, 8 GB RAM, 320 GB and 1000 GB hard drives, and a Nvidia Quadro FX 4800 graphic card, and it runs the current version of the 64-bit Arch Linux.

Preparation of Bank of Compounds. For our study, compounds from suppliers Asinex, ChemBridge, Maybridge, and the U.S. National Cancer Institute (NCI) were selected and downloaded from the ZINC database,²⁵ yielding 1.9 million compounds. A filtering procedure was

applied with the Filter program (OpenEye Scientific Software Inc.), and the choice of descriptors was the following:²⁶ molecular weight, 100–300 g/mol; number of ring systems, 1–3; number of H-bond donors, 0–4; number of H-bond acceptors, 0–6; number of rotatable bonds 0–5, and log *P*, –3.0 to 3.0. Additional filters were used to eliminate insoluble compounds (set to moderate) to eliminate all of the compounds containing atoms other than H, C, N, O, F, S, Cl, and Br and to eliminate all of the compounds with reactive functional groups. Also, a function developed by Shoichet and implemented in the Filter program was used to eliminate known and predicted aggregators.²⁷ The complete parameters used in the Filter program are available in Supporting Information p S26. The result from this filtering was a new subset of compounds containing roughly 143000 structures.

Molecular Docking. FlexX 3.1 (BiosolveIT GmbH)²⁸ was used for docking experiments. For docking to AKR1C1, the crystal structure with cocrystallized 3,5-dichlorosalicylic acid and NADP⁺ (PDB code: 3C3U)²³ was used, and for docking to AKR1C3, the crystal structure with cocrystallized indomethacin and NADP⁺ (PDB code: 1S2A)²⁹ was used. The active site was defined as the volume of the enzyme within 6 Å from cocrystallized ligand (3,5-dichlorosalicylic acid in AKR1C1 and indomethacin in AKR1C3). The cofactor NADP⁺ was retained in both structures. An essential interaction was defined in both cases so that only docked conformations with an H-bond acceptor within 3 Å from Tyr55 were considered. For the base placement, Triangle Matching was used; this program generated the maxima of 200 solutions per iteration and 200 per fragmentation. Both prepared structures were validated and FlexX was able to reproduce conformations of cocrystallized ligands.

All of the 143000 compounds from the filtering procedure were docked into active site of each AKR1C1 and AKR1C3 and ranked according to the score of the best scored conformation. From the compounds with the best scores from each docking experiment, 37 available compounds for AKR1C1 and 33 available compounds for AKR1C3 were obtained for *in vitro* evaluation from Maybridge, Chembridge, Asinex, and NCI.

Molecular Dynamics. As the initial structures for molecular dynamics in CHARMM, we used best-scored docked conformations of compound **26** in AKR1C1 and AKR1C3 with cofactor NADP⁺ in both protein structures. Molecular mechanics parameters for compound **26** were estimated using ParamChem tool and then optimized with Force Field Toolkit Plugin following instructions provided at <http://www.ku.uic.edu/Research/vmd/plugins/ftk>; Gaussian 09 was used to optimize geometry of compound **26** at the MP2/6-31G* level of theory. Missing hydrogens were added to the proteins prior to the minimization with the HBUILD tool in CHARMM. Steepest descent and adopted basis Newton–Raphson energy minimizations were performed to remove atomic clashes and to optimize the atomic coordinates of the protein–ligand complexes. The compound **26** was held fixed, and the two proteins were allowed to move freely during the minimization process. The docked complexes were then embedded in a cube of water, which was modeled explicitly by a rigid TIP3 model; KCl was added at a concentration of 0.35 M to neutralize the system. Trajectories of the AKR1C1 and AKR1C3 bound to compound **26** and NADP⁺ were generated at 37 °C and covered 10 ns of constant pressure and temperature molecular dynamics employing periodic boundary conditions. The first 3 ns of the molecular dynamics was heating (1 ns) and equilibration (2 ns); the analysis was performed using the final 7 ns of the simulation. No constraints were used during the simulation to allow the enzymes and the ligands to position themselves freely according to physical forces between them. The estimates of the binding free energy for compound **26** was calculated using the AutoDock docking program, which, in contrast to FlexX, allows scoring of individual conformations of bound molecules.

Inhibition Assays. Recombinant enzymes AKR1C1–AKR1C3 were prepared as described before.^{1,34} These enzymes *in vitro* catalyze the oxidation of the 1-acenaphthenol in the presence of the coenzyme NAD⁺, and this reaction was followed spectrophotometrically by measuring the increase in NADH absorbance ($\epsilon_{340} = 6220 \text{ M}^{-1}\text{cm}^{-1}$)

in the presence and absence of each of the compounds. The assays were carried out in a 0.3 mL volume that included 100 mM phosphate buffer (pH 9.0), 0.005% Triton X-114, and 5% DMSO as a cosolvent. A substrate concentration of 30 μM (K_m), 50 μM (K_m), and 100 μM ($<K_m$) and an enzyme concentration of 0.3, 0.2, and 1.5 μM were used for assays with AKR1C1, AKR1C2, and AKR1C3, respectively, in the presence of 2.3 mM coenzyme. Screening was performed at 400 μM compounds (or 200 μM in case of solubility problems). For compounds that showed more than 55% AKR1C1 and/or AKR1C3 inhibition, IC_{50} values were determined and selectivity toward AKR1C2 was measured. The measurements were performed on a Tecan Safire² and Biotek PowerWave XS microplate readers with initial velocities calculated, and the IC_{50} values were determined graphically from plots of \log_{10} [inhibitor concentration] versus % inhibition, using GraphPad Prism Version 4.00 (GraphPad Software, Inc.). K_i values were then calculated using the Cheng–Prusoff equation for competitive inhibition.

For the compounds **26** and **28**, we followed oxidation of *S*-tetralol by fluorometric measurement of NADPH formation using a Biotek Synergy 2 multi mode plate reader. The assay mixture was made up of 100 mM K_3PO_4 pH 7.0, 200 μM NADP^+ , *S*-tetralol (8 μM (K_m), 22.5 μM (K_m), 165 μM (K_m), and 75 μM (3 K_m) for AKR1C1, AKR1C2, AKR1C3, and AKR1C4 assay, respectively), inhibitor, and 111, 86, 95, and 184 nM AKR1C1–AKR1C4, respectively. Inhibitors were dissolved in DMSO to give final cosolvent concentration of 4% DMSO in a total reaction volume of 200 μL . The assay was conducted on a 96-well plate, and each inhibitor concentration was done in quadruplicate. The rate of *S*-tetralol oxidation was determined by calculation of initial velocity with the GENES software. Inhibition data were fit using Grafit 5.0 [$y = (\text{range}) / (1 + I / \text{IC}_{50})^s$] + background] to give the IC_{50} values.

Compound Characterization. The purity of compounds **3–6**, **9**, **11–17**, and **19–28** was determined using reversed-phase high-performance liquid chromatography (HPLC) analyses performed on an Agilent 1100 system (Agilent Technologies, Santa Clara, CA, USA) equipped with a quaternary pump and a multiple-wavelength detector using an Agilent Eclipse Plus C18, 5 μm (150 mm \times 4.6 mm) column. The compounds were dissolved in 40% acetonitrile/water at 0.16 mg/mL final concentration, and 5 μL was injected onto the column. Acetonitrile was used as an organic modifier, and 0.1% trifluoroacetic acid in water was used as an aqueous buffer. The elution was performed with a 1.0 mL/min flow rate using a linear gradient from 20% to 90% acetonitrile (10–90% for compound **25**) over 17 min, followed by 2.5 min at 90% acetonitrile, then back down to 20% acetonitrile over 30 s, and followed by 7 min of equilibration between samples. Detection was performed at 220 nm. The relative purity of compounds **3–5**, **9**, **12**, **15**, **16**, **19–22**, and **25–27** was above 95.0%. The relative purity of compounds **11**, **14**, and **17** was between 90 and 95%. The relative purity of compounds **6**, **13**, **23**, and **28** was between 80 and 90%.

¹H NMR spectra were recorded on a Bruker AVANCE III 400 MHz spectrometer in $\text{DMSO}-d_6$ solution, with tetramethylsilane as the internal standard. Mass spectra were obtained using a VG-Analytical Autospec Q mass spectrometer.

■ ASSOCIATED CONTENT

📄 Supporting Information

Results of biochemical characterization, docking ranks, and molecular weights of all compounds; compound characterization; parameters used with program Filter; similarity of known AKR1C inhibitors based on salicylic acid and amino-benzoic acid scaffolds to compounds **1–15**. This material is available free of charge via the Internet at <http://pubs.acs.org>.

■ AUTHOR INFORMATION

Corresponding Author

*Phone: +386-1-4769500. Fax: +386-1-4258031. E-mail: Stanislav.gobec@ffa.uni-lj.si

Author Contributions

[†]These authors contributed equally to this work.

Notes

The authors declare no competing financial interest.

■ ACKNOWLEDGMENTS

We thank OpenEye Scientific Software, Inc. for free academic licenses of their software and the Ministry of Higher Education, Science and Technology of the Republic of Slovenia for financial support. This study was partially supported by a young researcher grant to P.B. and J3-4135 grant to T.L.R., both from the Slovenian Research Agency, and by NIH grant 1R01-CA90744, P30-ES013508, and a Prostate Cancer Foundation award made to T.M.P.

■ ABBREVIATIONS USED

AKR, aldo-keto reductase; GABA, γ -aminobutyric acid; H-bond, hydrogen bond; MW, molecular weight; NAD(H), nicotinamide adenine dinucleotide; NADP(H), nicotinamide adenine dinucleotide phosphate; PG, prostaglandin

■ REFERENCES

- (1) Penning, T. M.; Burczynski, M. E.; Jez, J. M.; Hung, C. F.; Lin, H. K.; Ma, H.; Moore, M.; Palackal, N.; Ratnam, K. Human 3α -hydroxysteroid dehydrogenase isoforms (AKR1C1–AKR1C4) of the aldo-keto reductase superfamily: functional plasticity and tissue distribution reveals roles in the inactivation and formation of male and female sex hormones. *Biochem. J.* **2000**, *351*, 67–77.
- (2) Steckelbroeck, S.; Jin, Y.; Gopishetty, S.; Oyesanmi, B.; Penning, T. M. Human cytosolic 3α -hydroxysteroid dehydrogenases of the aldo-keto reductase superfamily display significant 3β -hydroxysteroid dehydrogenase activity: implications for steroid hormone metabolism and action. *J. Biol. Chem.* **2004**, *279*, 10784–10795.
- (3) Penning, T. M. Human hydroxysteroid dehydrogenases and pre-receptor regulation: insights into inhibitor design and evaluation. *J. Steroid Biochem. Mol. Biol.* **2011**, *125*, 46–56.
- (4) Brožič, P.; Turk, S.; Lanišnik Rižner, T.; Gobec, S. Inhibitors of aldo-keto reductases AKR1C1–AKR1C4. *Curr. Med. Chem.* **2011**, *18*, 2554–2565.
- (5) Penning, T. M.; Drury, J. E. Human aldo-keto reductases: function, gene regulation, and single nucleotide polymorphisms. *Arch. Biochem. Biophys.* **2007**, *464*, 241–250.
- (6) Penning, T. M.; Byrns, M. C. Steroid hormone transforming aldo-keto reductases and cancer. *Ann. N. Y. Acad. Sci.* **2009**, *1155*, 33–42.
- (7) Lanišnik Rižner, T.; Šmuc, T.; Ruprecht, R.; Šinkovec, J.; Penning, T. M. AKR1C1 and AKR1C3 may determine progesterone and estrogen ratios in endometrial cancer. *Mol. Cell. Endocrinol.* **2006**, *248*, 126–135.
- (8) Šmuc, T.; Hevir, N.; Ribič-Pucelj, M.; Husen, B.; Thole, H.; Lanišnik Rižner, T. Disturbed estrogen and progesterone action in ovarian endometriosis. *Mol. Cell. Endocrinol.* **2009**, *301*, 59–64.
- (9) Byrns, M. C.; Mindnich, R.; Duan, L.; Penning, T. M. Overexpression of aldo-keto reductase 1C3 (AKR1C3) in LNCaP cells diverts androgen metabolism towards testosterone resulting in resistance to the 5α -reductase inhibitor finasteride. *J. Steroid Biochem. Mol. Biol.* **2012**, *130*, 7–15.
- (10) Byrns, M. C.; Duan, L.; Lee, S. H.; Blair, I. A.; Penning, T. M. Aldo-keto reductase 1C3 expression in MCF-7 cells reveals roles in steroid hormone and prostaglandin metabolism that may explain its over-expression in breast cancer. *J. Steroid Biochem. Mol. Biol.* **2010**, *118*, 177–187.
- (11) Quinkler, M.; Bujalska, I. J.; Tomlinson, J. W.; Smith, D. M.; Stewart, P. M. Depot-specific prostaglandin synthesis in human adipose tissue: a novel possible mechanism of adipogenesis. *Gene* **2006**, *380*, 137–143.

- (12) Desmond, J. C.; Mountford, J. C.; Drayson, M. T.; Walker, E. A.; Hewison, M.; Ride, J. P.; Luong, Q. T.; Hayden, R. E.; Vanin, E. F.; Bunce, C. M. The aldo-keto reductase AKR1C3 is a novel suppressor of cell differentiation that provides a plausible target for the non-cyclooxygenase-dependent antineoplastic actions of nonsteroidal anti-inflammatory drugs. *Cancer Res.* **2003**, *63*, 505–512.
- (13) El-Kabbani, O.; Dhagat, U.; Hara, A. Inhibitors of human 20 α -hydroxysteroid dehydrogenase (AKR1C1). *J. Steroid Biochem. Mol. Biol.* **2011**, *125*, 105–111.
- (14) Byrns, M. C.; Jin, Y.; Penning, T. M. Inhibitors of type 5 17 β -hydroxysteroid dehydrogenase (AKR1C3): overview and structural insights. *J. Steroid Biochem. Mol. Biol.* **2011**, *125*, 95–104.
- (15) Byrns, M. C.; Steckelbroeck, S.; Penning, T. M. An indomethacin analogue, *N*-(4-chlorobenzoyl)-melatonin, is a selective inhibitor of aldo-keto reductase 1C3 (type 2 3 α -HSD, type 5 17 β -HSD, and prostaglandin F synthase), a potential target for the treatment of hormone dependent and hormone independent malignancies. *Biochem. Pharmacol.* **2008**, *75*, 484–493.
- (16) Bauman, D. R.; Rudnick, S. I.; Szweczek, L. M.; Jin, Y.; Gopishetty, S.; Penning, T. M. Development of nonsteroidal anti-inflammatory drug analogs and steroid carboxylates selective for human aldo-keto reductase isoforms: potential antineoplastic agents that work independently of cyclooxygenase isozymes. *Mol. Pharmacol.* **2005**, *67*, 60–68.
- (17) El-Kabbani, O.; Dhagat, U.; Soda, M.; Endo, S.; Matsunaga, T.; Hara, A. Probing the inhibitor selectivity pocket of human 20 α -hydroxysteroid dehydrogenase (AKR1C1) with X-ray crystallography and site-directed mutagenesis. *Bioorg. Med. Chem. Lett.* **2011**, *21*, 2564–2567.
- (18) Qiu, W.; Zhou, M.; Mazumdar, M.; Azzi, A.; Ghanmi, D.; Lu-The, V.; Labrie, F.; Lin, S.-X. Structure-based inhibitor design for an enzyme that binds different steroids: a potent inhibitor for human type 5 17 β -hydroxysteroid dehydrogenase. *J. Biol. Chem.* **2007**, *282*, 8368–8379.
- (19) El-Kabbani, O.; Scammells, P. J.; Day, T.; Dhagat, U.; Endo, S.; Matsunaga, T.; Soda, M.; Hara, A. Structure-based optimization and biological evaluation of human 20 α -hydroxysteroid dehydrogenase (AKR1C1) salicylic acid-based inhibitors. *Eur. J. Med. Chem.* **2010**, *45*, 5309–5317.
- (20) Adeniji, A. O.; Twenter, B. M.; Byrns, M. C.; Jin, Y.; Chen, M.; Winkler, J. D.; Penning, T. M. Development of potent and selective inhibitors of aldo-keto reductase 1C3 (type 5 17 β -hydroxysteroid dehydrogenase) based on *N*-phenyl-aminobenzoates and their structure–activity relationships. *J. Med. Chem.* **2012**, *55*, 2311–2323.
- (21) Adeniji, A. O.; Twenter, B. M.; Byrns, M. C.; Jin, Y.; Winkler, J. D.; Penning, T. M. Discovery of substituted 3-(phenylamino)benzoic acids as potent and selective inhibitors of type 5 17 β -hydroxysteroid dehydrogenase (AKR1C3). *Bioorg. Med. Chem. Lett.* **2011**, *21*, 1464–1468.
- (22) Brožič, P.; Turk, S.; Lanišnik Rižner, T.; Gobec, S. Discovery of new inhibitors of aldo-keto reductase 1C1 by structure-based virtual screening. *Mol. Cell. Endocrinol.* **2009**, *301*, 245–250.
- (23) Dhagat, U.; Carbone, V.; Chung, R. P.-T.; Matsunaga, T.; Endo, S.; Hara, A.; El-Kabbani, O. A salicylic acid-based analogue discovered from virtual screening as a potent inhibitor of human 20 α -hydroxysteroid dehydrogenase. *Med. Chem.* **2007**, *3*, 546–550.
- (24) Chessari, G.; Woodhead, A. J. From fragment to clinical candidate—a historical perspective. *Drug Discovery Today* **2009**, *14*, 668–675.
- (25) Irwin, J. J.; Shoichet, B. K. ZINC—a free database of commercially available compounds for virtual screening. *J. Chem. Inf. Model.* **2005**, *45*, 177–182.
- (26) Carr, R. A. E.; Congreve, M.; Murray, C. W.; Rees, D. C. Fragment-based lead discovery: leads by design. *Drug Discovery Today* **2005**, *10*, 987–992.
- (27) Shoichet, B. K. Interpreting steep dose–response curves in early inhibitor discovery. *J. Med. Chem.* **2006**, *49*, 7274–7277.
- (28) Rarey, M.; Kramer, B.; Lengauer, T.; Klebe, G. A fast flexible docking method using an incremental construction algorithm. *J. Mol. Biol.* **1996**, *261*, 470–489.
- (29) Lovering, A. L.; Ride, J. P.; Bunce, C. M.; Desmond, J. C.; Cummings, S. M.; White, S. A. Crystal structures of prostaglandin D(2) 11-ketoreductase (AKR1C3) in complex with the nonsteroidal anti-inflammatory drugs flufenamic acid and indomethacin. *Cancer Res.* **2004**, *64*, 1802–1810.
- (30) Penning, T. M.; Mukharji, I.; Barrows, S.; Talalay, P. Purification and properties of a 3 α -hydroxysteroid dehydrogenase of rat liver cytosol and its inhibition by anti-inflammatory drugs. *Biochem. J.* **1984**, *222*, 601–611.
- (31) Goodsell, D. S.; Morris, G. M.; Olson, A. J. Automated docking of flexible ligands: applications of AutoDock. *J. Mol. Recognit.* **1996**, *9*, 1–5.
- (32) Young, T.; Abel, R.; Kim, B.; Berne, B. J.; Friesner, R. A. Motifs for molecular recognition exploiting hydrophobic enclosure in protein–ligand binding. *Proc. Natl. Acad. Sci. U.S.A.* **2007**, *104*, 808–813.
- (33) Konc, J.; Janezic, D. ProBiS-2012: web server and web services for detection of structurally similar binding sites in proteins. *Nucleic Acids Res.* **2012**, *40*, W214–W221.
- (34) Brožič, P.; Šmuc, T.; Gobec, S.; Lanišnik Rižner, T. Phytoestrogens as inhibitors of the human progesterone metabolizing enzyme AKR1C1. *Mol. Cell. Endocrinol.* **2006**, *259*, 30–42.